Numerical Performance Analysis of Carbon Nanotube (CNT) Embedded MOSFETs

A. Akturk, G. Pennington, N. Goldsman

Department of Electrical and Computer Engineering University of Maryland,
College Park, MD 20742, USA
{akturka,garyp,neil}@glue.umd.edu

Abstract

We analyze a novel MOSFET design that has semiconducting single-walled zig-zag Carbon Nanotubes (CNTs) in the channel. We also report on a modeling technique for simulating CNT-MOSFET devices. Our investigations have shown that CNT-MOSFETs employing small diameter CNTs (d=8$\mathring{A}$) show low leakage and negative differential conductance. Midrange CNT-MOSFETs (d=13$\mathring{A}$) show improved current drive. However larger diameter CNTs (d=17$\mathring{A}$) result in degraded MOSFET performance due to effective punch-through and bandoffsets.

1 Device Model for CNT-MOSFETs

Recent experiments [1] and theoretical studies [2] indicate that semiconducting CNTs have the highest known mobility among semiconductors. Therefore CNTs have prompted large interest in research [1]-[5]. We here discuss models for numerical simulation of CNT embedded MOSFETs for feasibility analysis.

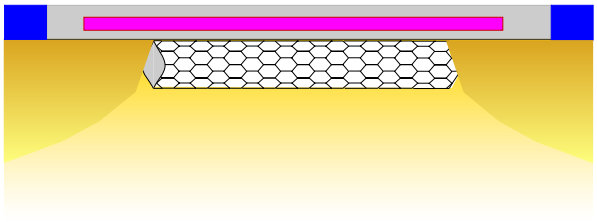

Figure 1: Proposed CNT-MOSFET.

We solve the Poisson equation along with modified electron-hole current continuity equations to obtain current-voltage characteristics of CNT-MOSFETs shown in Fig. 1. Our modified semiconductor equations account for quantum effects and band discontinuities. The complete set of equations is shown below:

$$\nabla^2\phi = -\frac{q}{\epsilon}(p - n + D) \quad (1)$$

$$\frac{\partial n}{\partial t} = \frac{1}{q}\nabla . J_n - R_n + G_n \quad (2)$$

$$\frac{\partial p}{\partial t} = -\frac{1}{q}\nabla . J_p - R_p + G_p \quad (3)$$

The electron current density J_n and hole current density J_p are defined as follows:

$$J_n = -qn\mu_n\nabla(\phi + \phi_{QM} + \phi_e) + q\mu_n V_{th}\nabla n \quad (4)$$

$$J_p = -qp\mu_p\nabla(\phi - \phi_{QM} - \phi_h) - q\mu_p V_{th}\nabla p \quad (5)$$

Here in addition to ϕ, we have effective potentials ϕ_{QM}, ϕ_e and ϕ_h to account for quantum and heterostructure effects.

1.1 Quantum Effective Potential

We use density gradient formalism to account for quantum confinement effects at the channel of MOSFET and at the band discontinuities between the CNT and silicon (Si). In this formalism quantum correction is defined as follows [6]:

$$\phi_{QM} = \frac{2\hbar^2}{12q\sqrt{n}}\left(\frac{1}{m_\parallel}\frac{\partial^2\sqrt{n}}{\partial x^2} + \frac{1}{m_\perp}\frac{\partial^2\sqrt{n}}{\partial y^2}\right) \quad (6)$$

Here x and y are parallel and perpendicular directions to the MOSFET channel. We set the effective mass to that of Si or CNT depending on the location.

1.2 CNT-Si Effective Potential

We also calculate the effects of conduction and valence band offsets on electrons and holes through ϕ_e and ϕ_h, respectively [7]. They account for the variations in bandgaps and electron affinities between Si and the CNT, and are expressed as:

$$\phi_e = \tfrac{1}{q}(\chi^{CNT} - \chi^{Si}) + V_{th}ln(\tfrac{n_o^{CNT}}{n_o^{Si}}) \quad (7)$$

$$= \tfrac{1}{q}\Delta E_C + V_{th}ln(\tfrac{n_o^{CNT}}{n_o^{Si}}) \quad (8)$$

$$\phi_h = -\tfrac{1}{q}(\chi^{CNT} - \chi^{Si} + E_G^{CNT} - E_G^{Si}) - V_{th}ln(\tfrac{n_o^{CNT}}{n_o^{Si}}) \quad (9)$$

$$= -\tfrac{1}{q}\Delta E_V - V_{th}ln(\tfrac{n_o^{CNT}}{n_o^{Si}}) \quad (10)$$

Here χ, n_o, E_G symbolize electron affinity, intrinsic carrier concentration and bandgap of Si and CNT, respectively. ΔE_C and ΔE_V are conduction and valence band discontinuities between Si and CNT. These effective potentials account for the contact resistance between Si and CNT which arises due to mismatch in the bandstructure.

1.3 Band Parameters of CNTs

To determine the electron affinity and bandgap of CNTs, we use the band diagram and electron affinity of graphite [2].
Our analyses indicate that bandgaps of semiconducting single-walled zig-zag CNTs are inversely proportional to their diameter. We here employ three different CNTs that have diameters (d) of $8\mathring{A}$, $13\mathring{A}$ and $17\mathring{A}$. These CNTs have the respective calculated bandgap values of 1.05eV, 0.67eV and 0.48eV. We later use these bandgap values to calculate CNT electron affinities. Corresponding CNT affinities are then the electron affinity of graphite (4.4eV [8]) minus half the bandgap value.

We next calculate the last term in the effective potential due to bandgap variations. Using nondegenerate statistics and the zero energy point at the midgap we obtained the following expression for the intrinsic carrier concentration of CNTs:

$$n_o^{CNT} = \sum_l \frac{1}{d^2} \sqrt{\frac{qV_{th}m^{*l}}{2\pi\hbar^2}} e^{-\frac{E^l}{qV_{th}}} \tag{11}$$

Here m^{*l} and E^l are CNT effective mass and energy in subband *l*, respectively.

1.4 Mobility Model for CNTs

We last need a mobility model to be used in the semiconductor equations. We employed a Monte Carlo (MC) simulator to obtain electron drift velocity versus electric field curves [2]. The simulations show high scattering rates for narrow CNTs, which allows for the extraction of mobility models. Our calculated velocity versus field curves show that CNTs attain very large drift velocities and show negative differential mobility (NDM). They are similar to GaAs in that respect, where conduction velocity of the first subband is larger than that of the second. We then developed an analytical model considering the lowest two subbands that give rise to the NDM effect. We next express the final mobility as a function of electric field and tube diameter using Mathiessen's rule:

$$\frac{1}{\mu(F,d)} = \frac{1}{\mu_1(F,d)} + \frac{1}{\mu_2(F,d)} \tag{12}$$

$$\mu_1(F,d) = \frac{\mu_o(d)}{1+\frac{F}{F_c(d)}} \tag{13}$$

$$\mu_2(F,d) = \frac{V_m(d)}{F(1+\lambda\frac{F}{F_c(d)})} \tag{14}$$

Here $\mu_o(d)$ is the low field CNT mobility and $F_c(d)$ is the electric field where CNT reaches peak drift velocity $V_m(d)$. Mobility of the second subband additionally includes an empirical parameter λ.

2 Simulation Results

We used the doping profile of a well-tempered MOSFET with channel length of 150nm. We then embed a planar sheet of CNTs at the topmost part of the channel of this MOSFET. We simulated three different CNTs with diameters of 8$\mathring{A}$, 13$\mathring{A}$ and 17$\mathring{A}$.
Figure 2 shows the current-voltage characteristics for V_{GS}= 1.0V. The CNT-MOSFET with the medium diameter tube has improved drive current capabilities largely due to the very high mobility in CNTs. However the biggest tubed CNT-MOSFET has degraded operation, with behavior that is more like a resistor. This can be attributed to the inability of MOSFETs with larger CNTs to form a pinchoff region. This may be related to the high intrinsic carrier concentration (roughly 10^{16} cm^{-3}) that is found in the largest tube. In addition, lowest diameter tubed device also operates like a MOSFET with drive currents slightly less than the conventional MOSFET under the specified conditions. The narrowest tubed device also shows inflection point towards high drain bias that can be related to the Schottky barrier between Si and CNT.

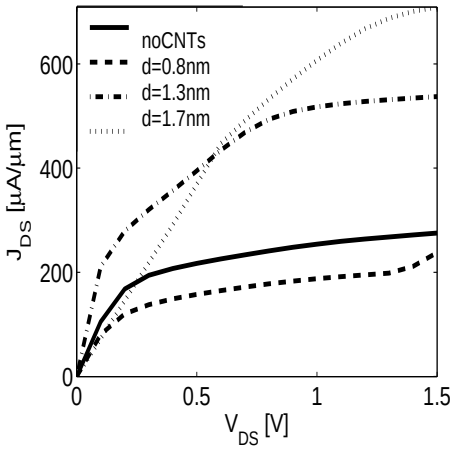

Figure 2: CNT-MOSFET current-voltage characteristics for V_{GS}=1.0V and different diameter CNTs.

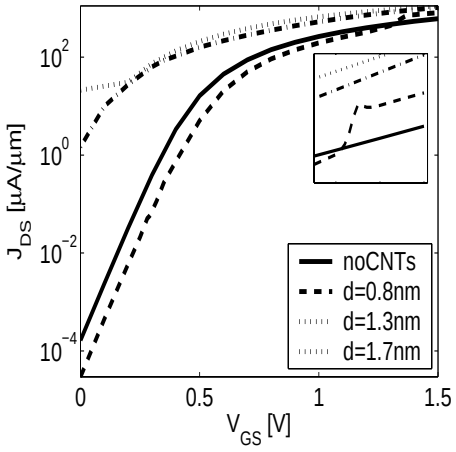

Figure 3: CNT-MOSFET drain currents for V_{DS}=1.2V. Inset is the linear scale plot around V_{GS}=1.36V.

We find that all CNT-MOSFETs show good subthreshold characteristics under low drain bias. However CNT-MOSFETs with larger diameter tubes start exhibiting leakier performance under high drain bias. Figure 3 shows the current-voltage characteristics for V_{DS}= 1.2V. For high drain bias the largest diameter CNT-MOSFET is very leaky. The MOSFET with the medium size tube also suffers drain induced barrier lowering which we associate it with the effects of the junction barrier between Si and CNT. The lowest diameter CNT-MOSFET performs best among all. In addition, the small diameter tube shows negative differential conductance that might be attributed to the barrier lowering at the Si-CNT junction and the effects of NDM.

In conclusion, simulations indicate that the CNT-MOSFET with small and medium diameter tubes show potentially improved performance over the conventional MOSFET. However performance degradation quickly sets in as the CNT diameter increases. In addition, CNT devices that use the NDM attribute of CNT mobility have the potential to be engineered for use in oscillators or related devices.

References

[1] T. Durkop, S. A. Getty, E. Cobas, M. S. Fuhrer, Nano Letters, vol. 4, pp. 35-39, 2004.

[2] G. Pennington, N. Goldsman, Phys. Rev. B., vol. 86, pp. 45426-45437, 2003.

[3] A. Akturk, G. Pennington, N. Goldsman, IEEE Conf. on Nanotech., pp. 24-27, 2003.

[4] R. Martel, V. Derycke, J. Appenzeller, S. Wind, Ph. Avouris, IEEE Design Auto. Conf., pp. 94-98, 2002.

[5] S. Heinze, J. Tersoff, R. Martel, V. Derycke, J. Appenzeller, Ph. Avouris, Phys. Rev. Letters, vol. 89, no. 10, pp. 106801-106804, 2002.

[6] J. R. Watling, A. R. Brown, A. Asenov, A. Svizhenko, M. P. Anantram, Sispad 2002, pp. 267-270, 2002.

[7] Y. Leblebici, S. Unlu, S-M. Kang, B. M. Onat, Jour. of Lightwave Tech., vol. 13, no. 3, pp. 396-405, 1995.

[8] A. Charlier, R. Setton, M-F. Charlier, Phys. Rev. B., vol. 55, no. 23, pp. 15537-15543, 1997.